PMSG Gear-Less Wind Turbine Equipped with an Active and Reactive Power supervisory

Othman B.k Hasnaoui **‡, Mehdi Allagui**, Jamel Belhadj **

*University of Tunis El Manar, LSE-ENIT B.P 37 le Belvédère 1002 Tunis Tunisia

*University of Tunis, ENSIT-DGE, B.P 56 Montfleury 1008 Tunis Tunisia

(mehdieep@yahoo.fr, Othmanbk.Hasnaoui@esstt.rnu.tn, Jamel.Belhadj@esstt.rnu.tn)

‡ Corresponding Author; Othman B.k Hasnaoui, University of Tunis, ENSIT-DGE, B.P 56 Montfleury 1008, Tunis, Tunisia, Othmanbk.Hasnaoui@esstt.rnu.tn

Received: 05.04.2014 Accepted: 12.05.2014

Abstract- In this paper, we present comparative studies related to some control techniques used to control high power permanent Magnet Synchronous Generator (PMSG) Gear-less Wind Turbines. For the two back-to-back converter (generator side and grid side), Field Oriented Control (FOC), Direct Torque Control (DTC), Voltage Oriented Control (VOC) and Direct Power Control (DPC) are investigated and compared according to many criteria (implementation complexity, steady state and transient performances). Control strategies are evaluated by simulation and are applied to a supervision scheme developed for a 2MW Direct Drive wind turbine. The scope is to verify the compliance of this system with E.On Netz german Grid Code including LVRT performances and active and reactive power management.

Keywords- Direct Drive, FOC, DTC, VOC, DPC, Supervisory control.

1. Introduction

Wind energy is a promising alternative to traditional energy sources [1]. Due to the increasing wind power penetration, the improvement of control strategies becomes a major challenge for manufacturers in order to comply with the grid connection requirements [2]. Consequently, new wind power plants are increasingly expected to provide ancillary services which maintain reliable operation of the interconnected transmission systems [3-4]. Compared to other wind turbine technologies, Direct Drive topology showed itself to be the most promising technique because it offers variable speed operation and fulfills GCR with high efficiency [5].

The power electronics subsystem is composed of two voltage source inverters (VSI) separately controlled. The generator-side converter controls the generator speed to maximize wind power extraction. On the other hand, grid-side converter (GSC) controls the dc-link voltage and the active and reactive power delivered to the grid connection point. For the two converters, direct control or vector control techniques can be used.

Permanent Magnets Synchronous Generator torque and the flux are intended to be controlled. On the other hand, control strategies for the GSC intend to decouple the reactive and active power supplied to the grid. To achieve these objectives, vector control techniques requires current control, in the rotating reference frame, and decoupling between the components so that the electromagnetic torque and power are indirectly controlled. In direct control strategies, the first step is to estimate torque and power. These two variables are then controlled directly, resulting in less complex and faster algorithms.

Consequently, it is relevant to evaluate the performance of vector and direct control techniques, in order to identify which is the most suitable control strategy. Therefore, in this work, FOC and DTC control strategies for the generator-side converter and VOC and DPC for the grid-side converter are considered.

The aim of this paper is to evaluate the performance of a PMSG-WT controlled by two different strategies for each power converter. In the first section, the wind turbine model is presented. The second section presents the control strategies of the generator-side convertor. Performances of

the two control techniques are simulated and analyzed. The third section presents the control strategies of the GSC with a comparative study. Finally, in the last section presents the developed supervision algorithm used to control reactive power. Transient stability of the wind system during grid faults are investigated for both control strategies.

2. Wind Turbine Structure

The wind turbine consists of the following components: A three-bladed rotor with the corresponding pitch angle controller; the MPPT algorithm; a PMSG with two back-to-back power converters, a DC-Link capacitor, and a grid LC-filter. The control of the PMSG-WT consists of two parts, the generator side control and the grid side control. The scheme of the wind turbine system is shown in Fig. 1.

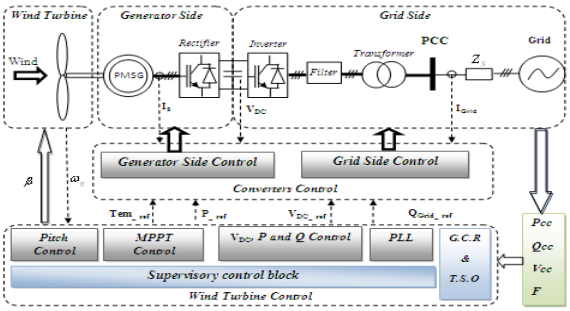

Fig.1. General Control scheme of PMSG-WT.

3. Direct Drive Wind Turbine Model

3.1. Aerodynamic model

The mechanical power produced by the wind turbine is expressed by [6]:

$$P_m = \frac{1}{2} C_p(\lambda, \beta).\rho.S.V_w^3 \quad (1)$$

In equation (1), C_p is the power coefficient, β is the pitch angle in degrees; ρ is the air density (kg/m3), S is the area swept by the blades (m²), V_w is the mean wind speed (m/s) and λ is the tip-speed-ratio given by:

$$\lambda = \frac{R.\Omega_g}{V_w} \quad (2)$$

Ω_g is the generator angular speed and is the turbine radius.

Fig. 2 shows the evolution mechanical power in function of the rotor speed for different wind speeds. The parabolic curve gives the optimal regime characteristic.

In this paper, the characteristic of the power coefficient ($C_p(\lambda,\beta)$) is approximated by the analytical equation (3). Details and parameters of this model are given in [7].

$$C_p(\lambda,\beta) = 0.22.(\frac{116}{\lambda_i} - 0.4\beta - 5).e^{\frac{-12.5}{\lambda_i}} \quad (3)$$

Where:

$$\lambda_i = \frac{1}{(\frac{1}{\lambda + 0.08\beta} - \frac{0.035}{\beta^3 + 1})} \quad (4)$$

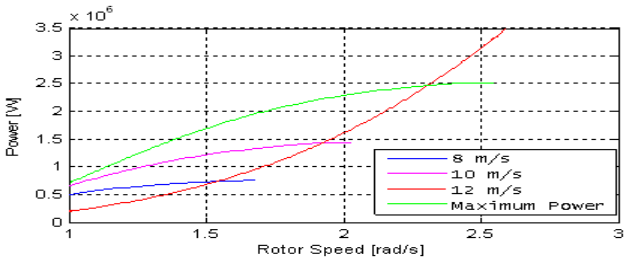

Fig. 2. Wind turbine power-speed curves.

3.2. Permanent magnets synchronous generator

The state equations of the PMSG are given below [8]:

$$\frac{d\phi_{sd}}{dt} = -r_s.I_{sd} + \omega_e.\phi_{sq} + V_{sd} \quad (5)$$

$$\frac{d\phi_{sq}}{dt} = -r_s.I_{sq} - \omega_e.\phi_{sd} + V_{sq} \quad (6)$$

In the above equations, the stator flux components are expressed by:

$$\phi_{sd} = L_{sd}.I_{sd} + \phi_v \quad (7)$$

$$\phi_{sq} = L_{sq}.I_{sq} \quad (8)$$

Where I_{sd}, I_{sq} and V_{sd}, V_{sq} are currents/voltages d and q axes, L_{sd} and L_{sq} are the stator inductances in the dq-reference frame, ω_e is the fundamental stator currents frequency, r_s is the stator windings resistance, and ϕ_v is the exciter flux of the PMSG. The electromagnetic torque of the generator is then given by:

$$T_{em} = \frac{3}{2} p(\phi_{sd}.I_{sq} - \phi_{sq}.I_{sd}) \quad (9)$$

p is the pairs pole number.

3.3. Voltage Source Inverter (VSI)

The Back-to-Back converter is widely used in wind turbine applications [9-10]. It uses a force-commutated rectifier and a force-commutated inverter each built of six insulated gate bipolar transistor (IGBT). The two converters

are connected through a common DC-link with a capacitor C_{dc} [9]. The DC-link capacitance C is chosen as [11],

$$C_{dc} = \frac{S}{4\Pi f_{\min} V_{dc} \Delta V_{dc}} \tag{10}$$

The generator side converter ensures variable speed operation of the wind turbine. The grid side converter is mainly used to control active and reactive powers delivered to the grid and to keep the DC-link voltage constant. The AC-side line-to-line RMS output voltage $U_{ll,RMS}$ is a function of the DC-link voltage V_{dc} and of the amplitude modulation ratio m [12],

$$U_{ll,RMS} = \frac{\sqrt{3}}{\sqrt{2}} m \frac{V_{dc}}{2} \tag{11}$$

With $0 \le m \le 1$.

The decoupling between the generator and the grid through power converters presents an important solution to comply with the G.C.R [13]. Figure 3 depicts the power electronics subsystem.

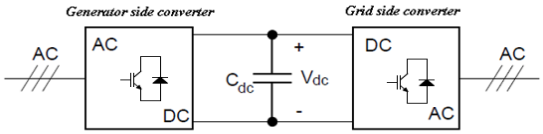

Fig.3. structure of Back-to-Back converter.

4. Generator side converter Control strategies

Two types of strategies exist for vector control, Field Oriented Control (FOC) and Direct Torque Control (DTC).

4.1. Field Oriented Control

FOC strategy is generally applied to the Generator-side converter (Fig. 4). It allows controlling the rotor speed through the control of the electromagnetic torque [14]. Torque control is achieved by setting to zero the d component of current and the torque is controlled through the q component. Details of this control strategy for variable pitch wind turbine and the MPPT algorithm are presented in [15].

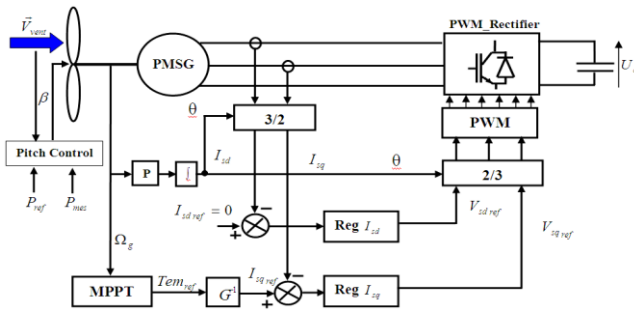

Fig.4. Block diagram of the Field Oriented Control (FOC).

4.2. Direct Torque Control

DTC principle consists of choosing a pre-defined switching table to select proper voltage vectors [16]. Vectors selection is based on stator flux linkage and the torque hysteresis control. In which case, the stator flux and the torque are controlled independently and directly. The torque hysteresis comparator is a three valued comparator. Whereas that, the flux hysteresis comparator is a two valued comparator. The control scheme of DTC is developed as shown in Fig. 5.

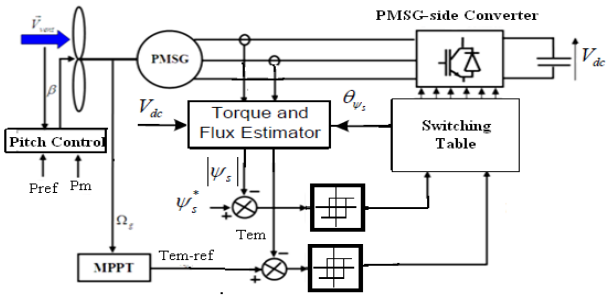

Fig.5. Direct Torque Control (DTC) block diagram.

4.3. Comparative study of DTC and FOC control

In order to compare the dynamic behavior the above control techniques, FOC and DTC responses are presented in Fig. 6. Simulations have shown that the FOC has higher torque ripple than DTC technique. Total Waveform Oscillation (Two) criteria is used to evaluate electromagnetic torque oscillation given by:

$$Two = \frac{\sqrt{T_{em-rms}^2 - T_{em-dc}^2}}{|T_{em-dc}|} * 100\% \tag{12}$$

Where T_{em-rms} and T_{em-dc} are the electromagnetic torque rms and average values, respectively.

Steady-state simulations show that the best power quality features and the smaller power-tracking error are given by the VOC technique. On the other hand, DTC technique offers the fastest transient behaviour without overshoot (~9%). Table 1 shows a brief description of simulation results along with the characteristics of each control strategies.

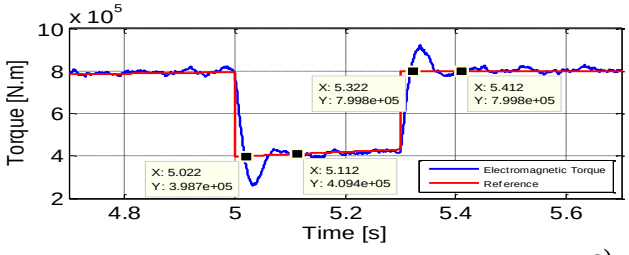

a)

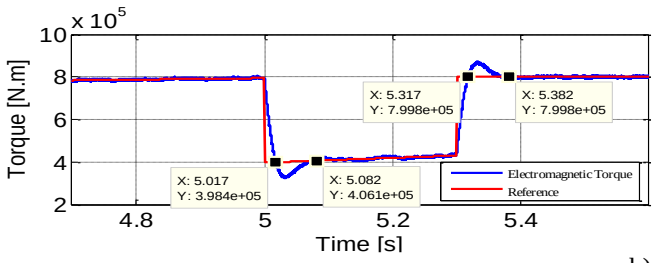

b)

Fig.6. PMSG time-domain waveforms Simulation results vs electromagnetic torque, during a load transient:

a) FOC technique; b) DTC technique.

Table.1. Control Features and Requirements for FOC and DTC control.

Features	*FOC*	*DTC*
Switching Frequency	*f = 2 kHz*	*f* = 5 kHz
Modulation Technique	PWM	Hysteresis
Current THD	*4.6%*	*11.2%*
Torque TWO	*1.34%*	*1.03%*
Cross-coupling Effect	*Yes*	*No*
Dynamic Performance	*Setting time (<112 ms)*	*Setting time (<82ms)*
	Rise time (<22 ms)	*Rise time (<17 ms)*
	Overshoot (~24%)	*Overshoot (~9%)*

5. Grid Side Converter Control strategies

5.1. Voltage Oriented Control (VOC)

The grid side converter is mainly used to control active and reactive powers delivered to the grid, in order to keep the DC Link voltage constant, and to ensure the quality of the injected power. Voltage Oriented Control requires internal current control loops in the rotating dq frame and the elimination of the current cross coupling between the d and q components. The connection to the grid is achieved through an LCL filter and a transformer. The Phased Locked Loop (PLL) gives an estimation of θ_s, the angle of the grid voltage. In this way, an accurate synchronization between the inverter voltage and the voltage at the PCC is obtained. The PLL technique is detailed in [15]. Grid synchronization, DC-link voltage control, and reactive / active power supplied to the grid, are shown in Fig. 7.

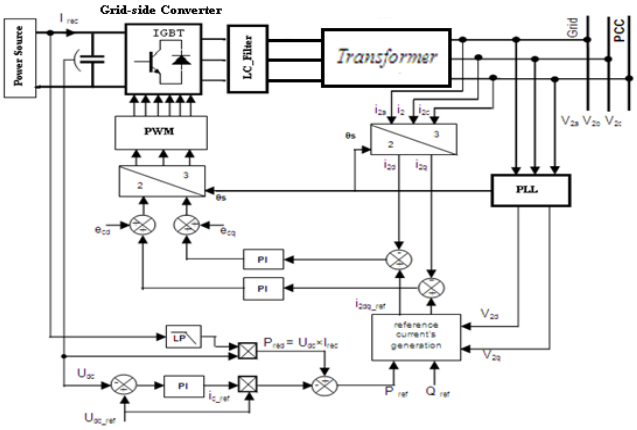

Fig.7. Block diagram of the Voltage Oriented Control (VOC) technique.

5.2. Direct Power Control (DPC

Conventional direct power control allows to directly controlling active and reactive powers using a switching table. It uses the same principle of DTC. Conventional DPC is characterized by the high ripple in grid currents which gives a poor power quality [17]. In addition, the switching frequency is not controlled, which increase the difficulty for correct harmonic filter design. Consequently, conventional DPC is combined with SVM technique to obtain constant switching frequency and low current distortion [18]. The developed DPC for the grid-side converter is shown in Fig. 8. In this figure, the unity power factor is obtained by setting the reactive power reference Q* to zero.

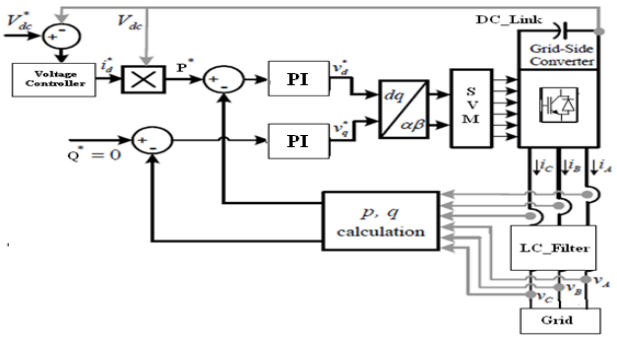

Fig.8. Block diagram of the Direct Power Control (DPC) technique.

5.3. Comparative study of DPC and VOC control

The steady-state is evaluated by means of current THD measurements, active and reactive power ripple values (ΔP , ΔQ) and some DC-link performance features as the voltage ripple ΔV_{DC}. On the other hand, the cross-coupling effect and the typical dynamic performance criterions as the settling time, rise time and overshoot are considered in the transient-state operation.

5.3.1. Steady-state Performance

Fig. 9 and Fig. 10 show the per-phase switching signals, grid currents, spectrum analysis and power performance for the grid side converter, using both the VOC-type control strategy and the DPC techniques. As can be observed the VOC control shows the best power quality (THD=2.3%) and the minimum power ripple ($\Delta P = 8\%$, $\Delta Q = 9.2\%$). The DPC control leads to a dispersed harmonic spectrum with a large THD of around 9% with considerable power ripple values ($\Delta P = 17.6\%$, $\Delta Q = 19.4\%$).

According to the IEEE standards 519-1992 recommendation, the limit of harmonic distortions for distributed power systems connected to the grid should not exceed 5% [19]. In this way, only VOC meets the grid connection requirements (GCR). On the other hand, the VOC strategy shows a small tracking error of around 0.32%, while the absolute tracking error reaches 4% in the DPC case. Furthermore, the voltage ripple in the DC-link capacitor is clearly smaller in the VOC ($\Delta V_{DC} = 5\%$) than the DPC strategy ($\Delta V_{DC} = 14\%$), see figure 11.

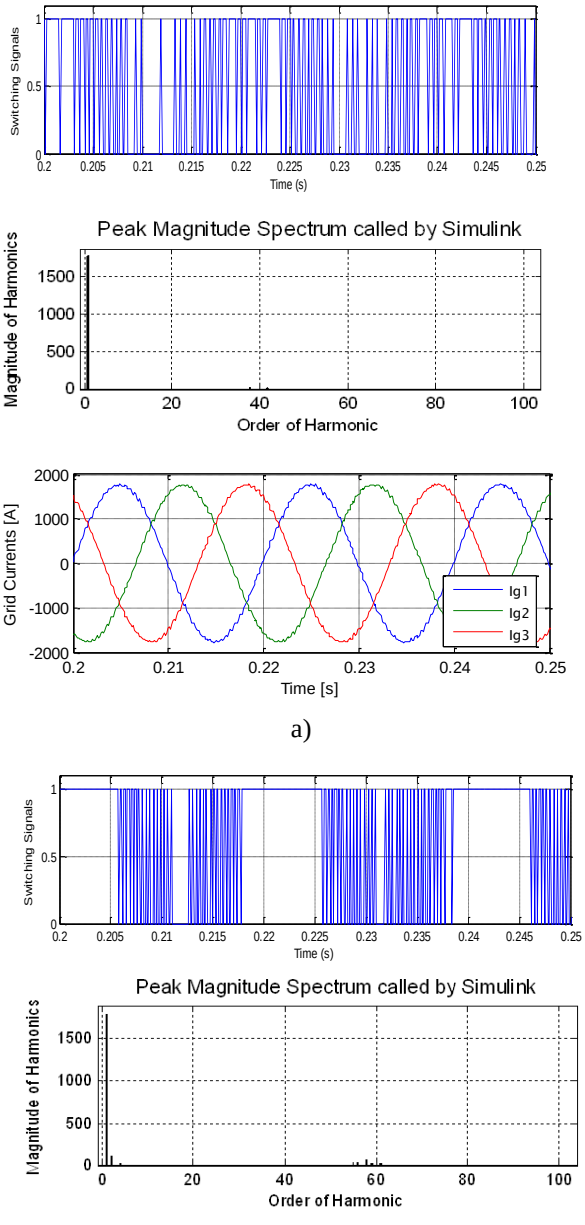

a)

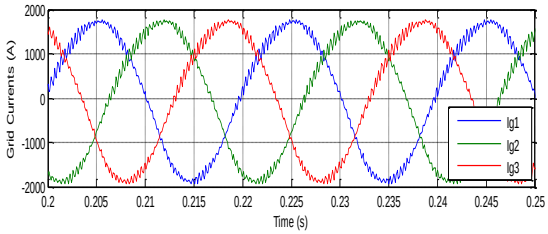

b)

Fig.9. Phase switching signals, grid currents and spectrum analysis: a) VOC Techniques b) DPC Techniques.

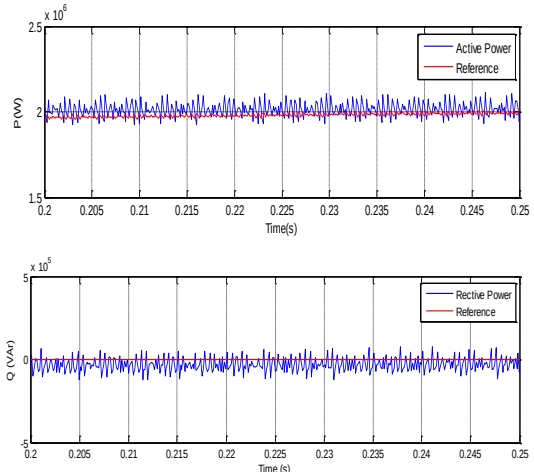

a)

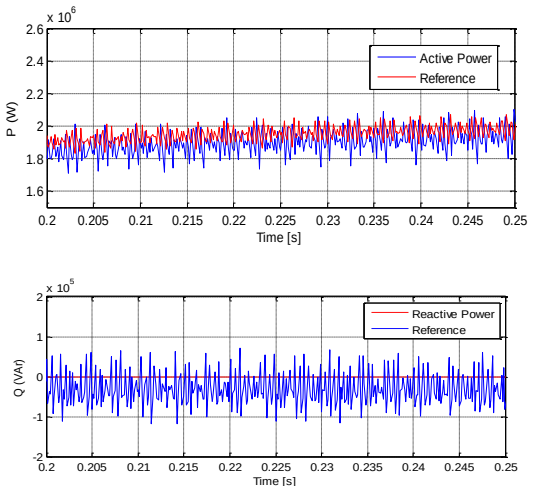

b)

Fig.10. Active and reactive power behaviors: a) VOC Techniques b) DPC Techniques.

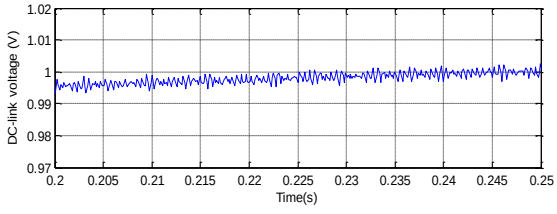

a)

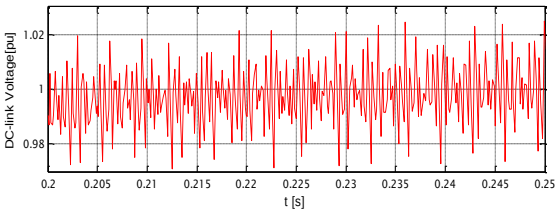

b)

Fig.11. DC-link voltage: a) VOC Techniques b) DPC Techniques.

5.3.2. Transient Performances

Several simulations have been carried out in order to verify the behavior of the proposed control algorithms during transients operation. These simulations involve the grid side converter configurations with the VOC and DPC-based control strategies. Active-power reference steps from 1.4MW to 2MW have been applied (30% of nominal power). Note that reactive power steps will produce similar results in transients, so these cases are not evaluated. Figure 12 shows the instantaneous active and reactive power behavior during active reference steps. As shown, the DPC technique is clearly faster than the VOC techniques in power tracking task. The transient performance shows the expected behavior in the VOC-based strategy (Fig. 13).

To quantify the transient behavior, a power band near 5% of the rated power is established. In this way, a setting time close to 60.6ms, a rise time below 17.2 ms and a small overshoot of around 25% can be observed in the VOC-based configuration. Yet, the DPC needs a setting time below 44.8ms with a rise time of around 13ms without overshoot (~5%) in power tracking requirements. Furthermore, there is no cross-coupling effect between active and reactive power in the DPC, whereas the VOC shows a substantial perturbation in the reactive power behavior when active power changes are applied.to the IEEE standards 519-1992 recommendation

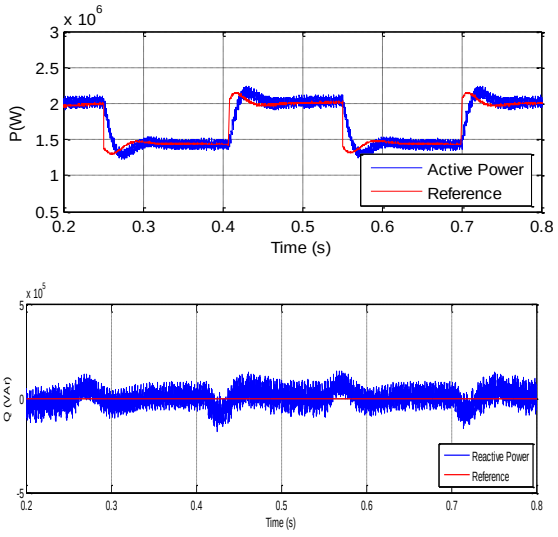

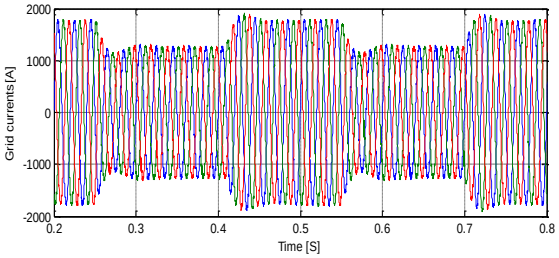

a)

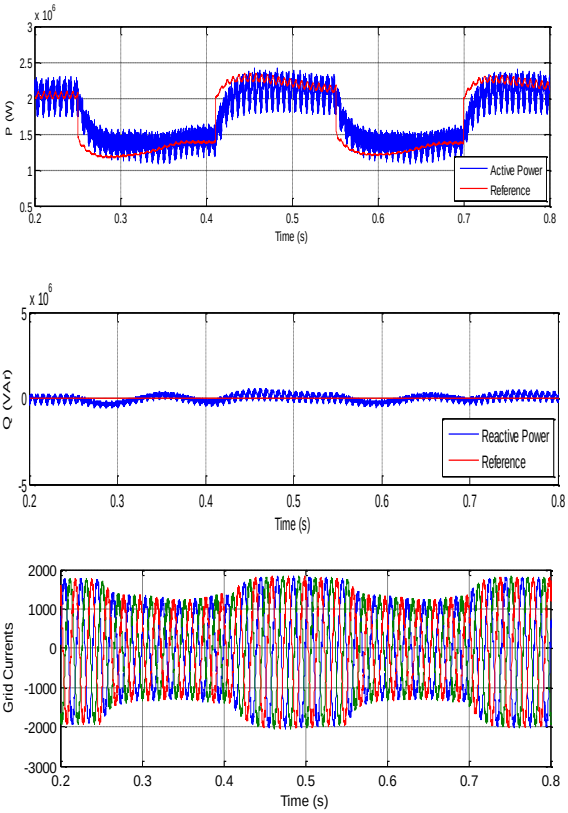

b)

Fig.12. Instantaneous active and reactive power behaviors during active reference steps: a) VOC Techniques b) DPC Techniques.

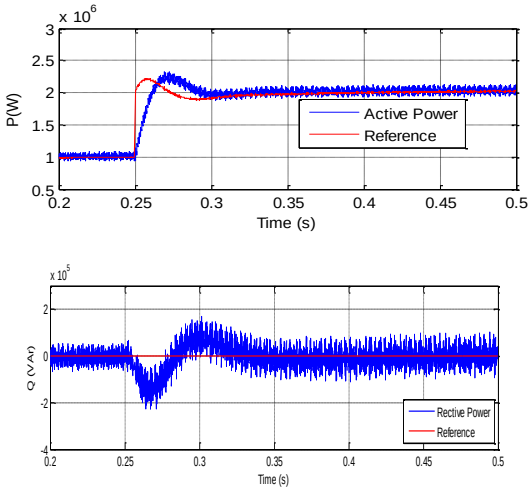

a)

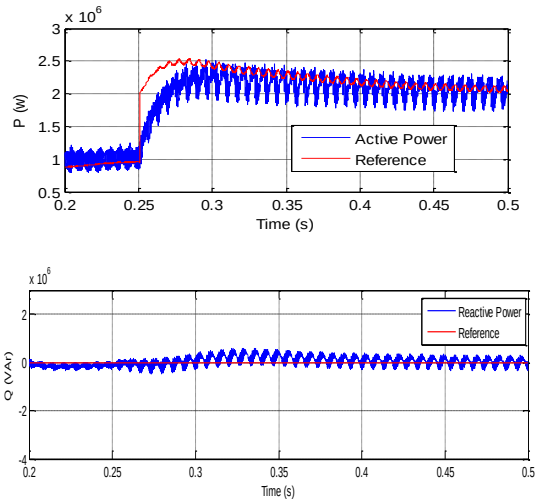

b)

Fig.13. Active and reactive power transient behaviors:

a) VOC Techniques b) DPC Techniques

The steady-state simulations show the best power quality features and the smaller power-tracking error are obtained with VOC techniques. On the other hand, DPC -based strategies offer the fastest transient behavior without overshoot and cross-coupling effect. Table 2 shows a brief description of the simulation results along with the characteristics and requirements of each control strategy. Consequently, It is concluded that combination of vector and direct control represent the best choice, depending on the desired performance tradeoff.

Table.2. Control Features and Requirements for VOC and DPC techniques

Features	*VOC*	*DPC*
Switching Frequency	*f = 2 kHz*	*f = 5 kHz*
Modulation Technique	*PWM*	*SVM*
Current THD	*2.3%*	*8.77%*
Power Ripple	ΔP *(8%)* ΔQ *(9.2%)*	ΔP *(17.6%)* ΔQ *(19.4%)*
DC-link Ripple	ΔV_{DC} *(5%)*	ΔV_{DC} *(14%)*
Cross-coupling Effect	*Yes*	*No*
Dynamic Performance	*Setting time (<60.6ms)*	*Setting time (<44.8ms)*
	Rise time (<17.2ms)	*Rise time (<13.3ms)*
	Overshoot (~25%)	*Overshoot (~5%)*

6. Reactive power control supervisory

6.1. Low Voltage Ride Through (LVRT) capabilities and voltage grid support

Currently, wind turbines should stay connected to the grid in the case of voltage dips [20]. This is of particular importance to the TSOs, since wind farms disconnection could cause major loss of power generation and consequently, power system instability [3-21]. Grid connection requirements used in this paper are those defined by the TSO E.ON and presented in Fig. 14 [3].

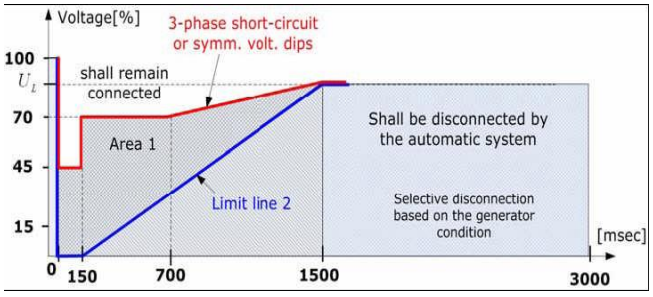

Fig. 14. LVRT Voltage profile according to [3].

Reactive power supervisory control presented below is to regulate the specified PCC voltage (Fig. 15). According to the GCR of the German operator E. ON Netz, wind farms should support the grid voltage during faults. To achieve this target, Grid side converter must supply reactive current equivalent to 2% In per 1% Un voltage dip. Thus, supervisory control block contains two control levels which are activated according to the dip magnitude:

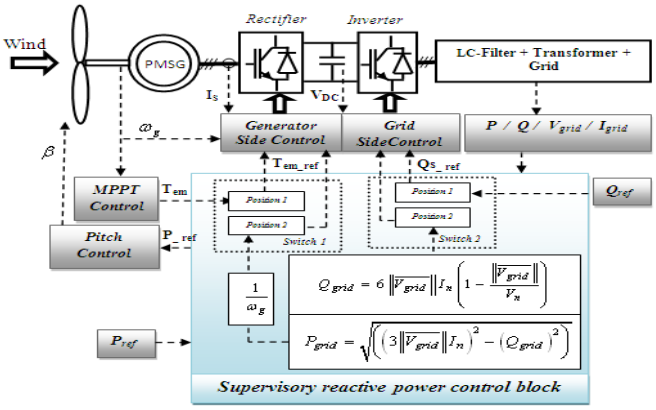

Fig.15. Schematic diagram of the reactive power supervisory.

- ***Level 1:*** $\left\|\overline{V_{grid}}\right\| \geq 50\%V_n$: In this condition, the normal operating mode is activated. The torque reference T_{em_ref} is given by the MPPT algorithm and power production is optimized. Reactive power reference is fixed by the TSOs.
- ***Level 2:*** $\left\|\overline{V_{grid}}\right\| \leq 50\%V_n$: During faults, the wind turbine should supply reactive currents to the grid. Therefore, reactive power reference Q_{grid} is calculated by:

$$Q_{grid} = 6\left\|\overline{V_{grid}}\right\| I_n \left(1 - \frac{\left\|\overline{V_{grid}}\right\|}{V_n}\right) \quad (13)$$

Then, Q_{grid} is used to calculate active power reference P_{grid} given by (14):

$$P_{grid} = \sqrt{\left(\left(3\left\|\overline{V_{grid}}\right\| I_n\right)^2 - \left(Q_{grid}\right)^2\right)} \quad (14)$$

The calculated power P_{grid} should be available at the output of the generator side converter. Therefore, when a voltage dip is detected, torque reference switches to another value given by (15):

$$T_{em-ref} = \frac{P_{grid}}{\omega_g} \quad (15)$$

6.2. *Comparative study of DPC and VOC control*

Fig. 16 and 17 show the response of the both control strategy to a symmetrical voltage dip. The dip magnitude is divided in two part; 45% then 70% of the rated voltage, as illustrated in Figure 15.

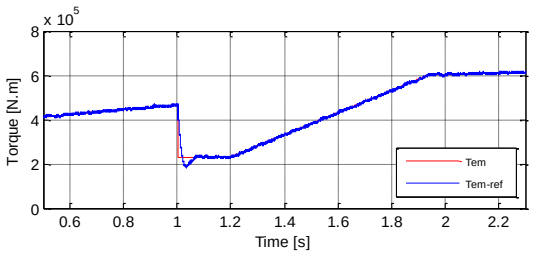

Fig. 16. Wind turbine behavior during a symmetrical fault (type A), with the VOC Techniques.

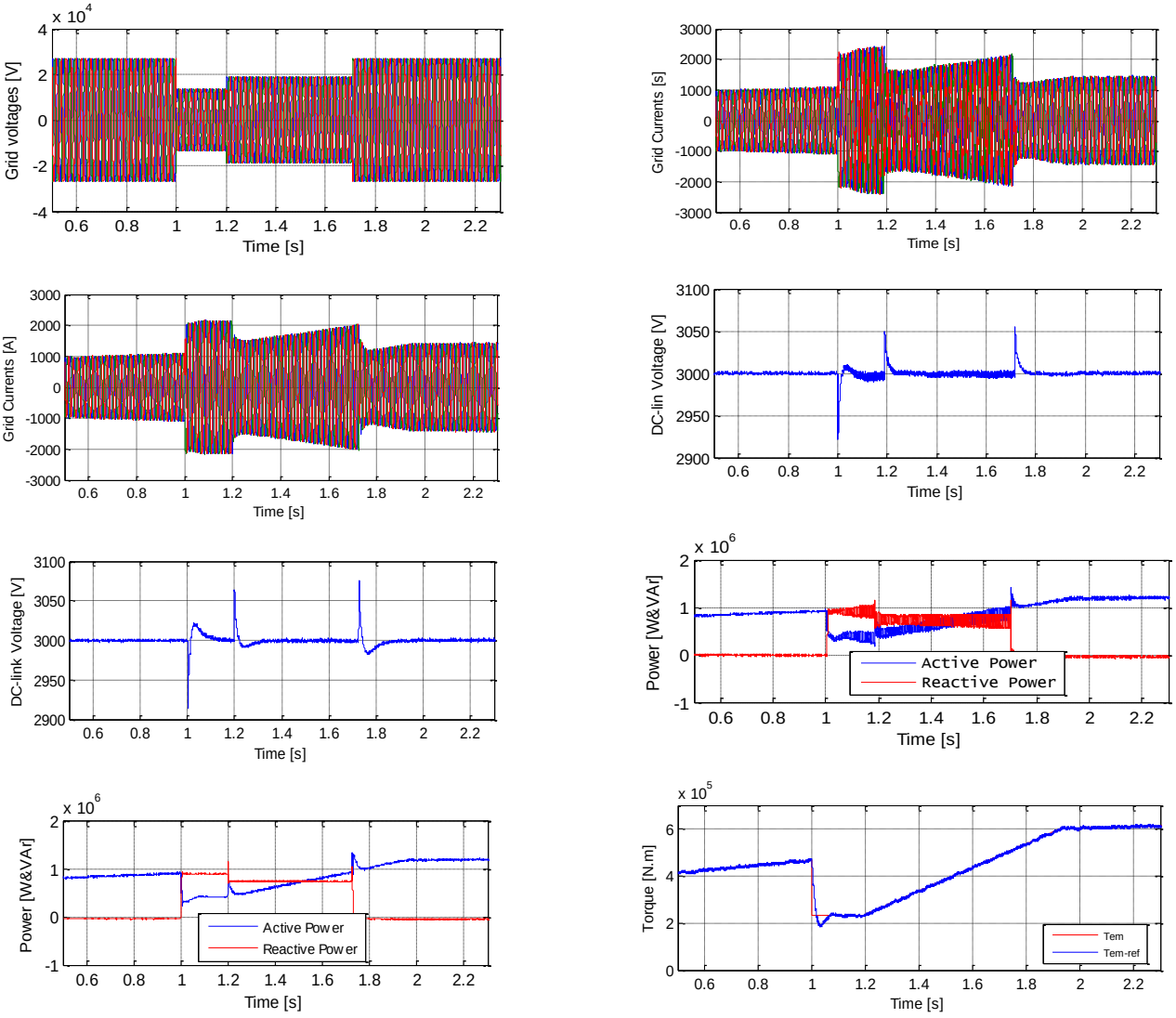

Fig. 17. Wind turbine behavior during a symmetrical fault (type A), with the DPC Techniques.

This result shows that DC-link voltage is weakly affected and remains within 10% of allowed limits. For both control techniques, PMSG doesn't disconnect from the grid but continue to inject reactive power in order to support the grid with control of reactive current value in order to save the back-to-back converters; while the active power is decreased with a gradient of 20% per second of rated power to comply with Grid Connection Requirements. It is noticed that rotor speed is no longer controlled during the fault since torque reference is not taken from the MPPT algorithm. Finally, vector control technique (VOC) is characterized by a lower harmonic distortion THD and higher efficiency. On the other hand, DTC is less computational demanding and it gives a better dynamic response.

7. Conclusion

The synthesis and analysis of two different control strategies for PMSG-WT have been carried out. The results of this comparative study show that all control strategies can be used to control direct drive wind turbines. However, the best power quality features and the smaller power-tracking error are obtained with vector control techniques. On the other hand, direct control offers the better dynamic response without overshoot and cross-coupling effect.

According to the simulation results, the wind turbine does not trip during a grid fault. In addition it delivers reactive power to support the grid voltage. Thus, supervisor performances comply with the GCR for both control strategies. We note that the vector control is more adapted, and direct control responses are quicker.

Appendix

Wind Turbine Parameters
$P = 2MW$
$N_m = 24rpm$
$J_{tot} = 6.2.10^6 kg.m^2$
$D = 75m$
3 Blades
Variable Speed
Collective Pitch

PMSG parameters
$P_{nom} = 2.02MW$
$U_{nom} = 1.75kV$
$I_s = 660A$
$r_s = 3.2m\Omega$
$L_{sd} = 2.7mH$
$L_{sq} = 1.7mH$
$\phi_v = 18.6wb$
$p = 32$

Grid side Converter Parameters
$S = 2MW$
$U_{dc} = 3kV$
$C_{dc} = 20mF$
$R_g = 0.3m\Omega$
$L_g = 0.01mH$
$C_f = 35\mu F$

References

[1] The European Wind Energy Association. Gwec - table and statistics 2009, December 2010. http://www.ewea.org.

[2] Gabriele Michalke, "Variable Speed Wind Turbines -Modeling, Control, and Impact on Power Systems", PhD thesis, Department of Renewable Energies at Darmstadt Technical University (Germany), 2008.

[3] F. Lov, A. Daniela Hansen, P. Sørensen and N. Antonio Cutululis, "Mapping of grid faults and grid codes", Technical University of Denmark, Vol: Risø-R-1617(EN), Publisher: Risø National Laboratory, Roskilde Denmark, July 2007.

[4] S. Heier, "Grid integration of wind energy conversion systems", John Wiley & Sons Ltd, 2nd ed.,Chichester, UK, 2006.

[5] V. Akhmatov, "Modelling and Ride-through Capabilities of Variable Speed Wind Turbines With Permanent Magnet Generators", Wiley Interscience, Vol 1, pp1-14 ,2005.

[6] F. D. Bianchi, H. De Battista, R. J. Mantz, "Wind Turbine Control Systems", Springer, England, 2007.

[7] S. Heier, "Grid integration of wind energy conversion systems", Chichester: John Wiley & Sons Ltd, pp.35-302, 1998.

[8] H. Woo Kim, Sung-Soo Kim, Hee-Sang Ko, "Modeling and control of PMSG-based variable-speed wind turbine", Electric Power Systems Research, vol. 80, 46-52, 2010.

[9] A. Carlsson, "The back-to-back converter", Thesis, Lund Institute of Technology, Lund, Sweden, May 1998.

[10] R. Pena, J.C. Clare and G.M. Asher, "Doubly-fed induction generator using back-to-back PWM converters and its application to variable speed wind energy generation", IEEE proceedings on electronic power application, 143(3), 231-241, 1996.

[11] G. Michalke, Variable Speed Wind Turbines, "Modeling, Control, and Impact on Power Systems," PhD Thesis, Darmstadt Technical University, Germany, 2008.

[12] L. Quéval, "Modeling and simulation of grid connected superconducting wind turbine generators", Ph.D.Thesis, the University of Tokyo, Department of advanced energy, (Tokyo), 2013.

[13] M. Chinchilla, S. Arnaltes, and J. Burgos, "Control of permanent-magnet generators applied to variable-speed wind-energy systems connected to the grid", IEEE Transactions on energy conversion, vol. 21, p. 6, 2006.

[14] E. Mahersi, A. Khedher, M.F. Mimouni, "The Wind energy Conversion System Using PMSG Controlled by Vector Control and SMC Strategies", International Journal of Renewable Energy Research (IJRER), Vol.3, No.1, pp: 41-50, 2013.

[15] M. Allagui, O.B.k. Hasnaoui and J. Belhadj, "Exploitation of pitch control to improve the integration of a direct drive wind turbine to the grid", Journal of Electrical Systems, 9(2), 179-190, 2013.

[16] M. F. Rahman, L. Zhong, E. Haque, and M. A. Rahman, "A Direct Torque-Controlled Interior

Permanent-Magnet Synchronous Motor Drive Without a Speed Sensor ", IEEE Trans. Energy conversion, vol. 18, no. 1, Mar. 2003.

[17] G. Escobar, A. M. Stankovic, J. M. Carrasco, E. Galvan, and R. Ortega, "Analysis and design of direct power control (DPC) for a three phase synchronous rectifier via output regulation subspaces," IEEE Transactions on Power Electronics, vol. 18, no. 3, pp. 823-830, May,2003.

[18] M. Malinowski, M. Jasinski, and M. P. Kazmierkowski, "Simple direct power control of threephase PWM rectifier using space-vector modulation (DPC-SVM)", IEEE Transactions on Industrial Electronics, vol. 51, no. 2, pp. 447-454, Apr.2004.

[19] IEEE 519 working Group, IEEE Recommended Practices and Requirements for Harmonic Control in Electrical Power Systems, IEEE STD 519-1992, 1992.

[20] J.S. Lather, S.S Dhillon, S.Marwaha, "Modern control aspects in doubly fed induction generator based power systems", A review, International Journal of Advanced Research in Electrical, Electronics and Instrumentation Engineering, Vol. 2, Issue 6, June 2013.

[21] E.ON Netz GmbH, Netzanschlussregeln für Hoch- und Höchstspannung, April 2006.ference»